JACC Vol. 32, No. 7
December 1998:2072–9

Adventitial Vasa Vasorum in Balloon-injured Coronary Arteries

Visualization and Quantitation by a Microscopic Three-dimensional Computed Tomography Technique

HYUCK MOON KWON, MD, GIUSEPPE SANGIORGI, MD, ERIK L. RITMAN, MD, PHD,*
AMIR LERMAN, MD, CHARLES MCKENNA, MD, RENU VIRMANI, MD,‡
WILLIAM D. EDWARDS, MD,† DAVID R. HOLMES, MD, ROBERT S. SCHWARTZ, MD
Rochester, Minnesota and Washington, DC

Objectives. **The objective of this study was to examine the quantitative response of the adventitial vasa vasorum to balloon-induced coronary injury.**

Background. **Recent attention has focused on the role of vasa vasorum in atherosclerotic and restenotic coronary artery disease. However, the three-dimensional anatomy of these complex vessels is largely unknown, especially after angioplasty injury. The purpose of this study was to visualize and quantitate three-dimensional spatial patterns of vasa vasorum in normal and balloon injured porcine coronary arteries. We also studied the spatial growth of vasa vasorum in regions of neointimal formation. A novel imaging technique, microscopic computed tomography, was used for these studies.**

Methods. **Four pigs were killed 28 d after coronary balloon injury, and four pigs with uninjured coronary arteries served as normal controls. The coronary arteries were injected with a low-viscosity, radiopaque liquid polymer compound. Normal and injured coronary segments were scanned using a microscopic computed tomography technique. Three-dimensional reconstructed maximum intensity projection and voxel gradient shading images were displayed at different angles and voxel threshold values, using image analysis software. For quantitation, seven to 10 cross-sectional images (40 normal and 32 balloon injured cross-sections) were captured from each specimen at a voxel size of 21 μm.**

Results. **Normal vasa vasorum originated from the coronary artery lumen, principally at large branch points. Two different types of vasa were found and classified as first-order or second-order according to location and direction. In balloon-injured coronary arteries, adventitial vasa vasorum density was increased ($3.16 \pm 0.17/mm^2$ vs. $1.90 \pm 0.06/mm^2$, $p = 0.0001$; respectively), suggesting neovascularization by 28 d after vessel injury. Also, in these injured arteries, the vasa spatial distribution was disrupted compared with normal vessels, with proportionally more second-order vasa vasorum. The diameters of first-order and second-order vasa were smaller in normal compared with balloon-treated coronary arteries ($p = 0.012$ first-order; $p < 0.001$, second-order; respectively). The density of newly formed vasa vasorum was proportional to vessel stenosis ($r = 0.81$, $p = 0.0001$). Although the total number of vasa was increased after injury, the total vascular area comprised of vasa was significantly reduced in injured vessels compared with normals ($3.83 \pm 0.20\%$ to $5.42 \pm 0.56\%$, $p = 0.0185$).**

Conclusions. **Adventitial neovascularization occurs after balloon injury. The number of new vessels is proportional to vessel stenosis. These findings may hold substantial implications for the therapy of vascular disease and restenosis.**

(J Am Coll Cardiol 1998;32:2072–9)

The adventitia in normal coronary arteries contains a fine network of microvasculature that provide oxygen and nutrients to the outer layers of the arterial wall. The three-dimensional (3-D) anatomy and function of these small vessels is not well defined (1), yet growing experimental evidence suggests an association with neointimal formation (2). Studies have shown that coronary atherosclerosis is associated with increased numbers of vasa vasorum, both in the adventitia and in the plaque itself (2–4). This may relate to the observation that angiogenic factors (5,6) and adhesion molecules (7,8) are also vascular smooth muscle cell and endothelial cell mitogens.

See page 2080

Since balloon angioplasty produces its effect by intimal splitting and disruption of the vessel wall, damage to the adventitia layer occurs as well (9–11). Balloon injury stimu-

From the Department of Internal Medicine and Cardiovascular Diseases, *Department of Physiology and Biophysics, and †Division of Medical Pathology, Mayo Clinic and Mayo Foundation, Rochester, Minnesota; and ‡Department of Cardiovascular Pathology, Armed Force Institute of Pathology, Washington, DC. This study was supported in part by the J. Holden DeHaan Foundation, Naples, FL, and the National Institutes of Health (RR-11800).

Manuscript received October 28, 1997; revised manuscript received July 1, 1998, accepted August 20, 1998.

Address for correspondence: Robert S. Schwartz, MD, Department of Cardiovascular Diseases, Mayo Clinic, 200 First St., SW, Rochester, MN 55905. E-mail: schwartzr@mayo.edu.

Published by Elsevier Science Inc.

0735-1097/98/$19.00
PII S0735-1097(98)00482-3

Abbreviations and Acronyms

CT = computed tomography
PTCA = coronary angioplasty
3D = three-dimensional

lates the growth of neointimal hyperplasia, but its effects on adventitial neovascularization are less clear (2,12,13). Vasa formation may thus play a role in the pathogenesis of neointimal hyperplasia and restenosis in injured coronary arteries (14,15). It is unclear, however, whether angiogenesis enhances or inhibits neointimal formation. We therefore examined and quantitated the 3-D spatial patterns of vasa vasorum in normal and balloon-injured porcine coronary arteries, and delineated the spatial distribution of vasa related to neointimal formation using a new microscopic 3-D computed tomography imaging technique.

Methods

Balloon injury. All animal studies were approved by the Mayo Clinic Institutional Animal Care and Use Committee. Eight juvenile, domestic, crossbred swine were fed a normal laboratory chow diet without cholesterol supplementation. Ketamine (30 mg/Kg body weight) and Xylazine (3 mg/Kg) were given intramuscularly for general anesthesia. Atropine (1 mg) was used intramuscularly to decrease oropharyngeal secretions, and Flocillin (1 g) was given prophylactically for infection.

Arterial access was obtained through carotid artery cutdown. The right external carotid artery was exposed, and an 8F hemostatic sheath placed for arterial access. A single heparin bolus (10,000 units) was administered through the sheath. Coronary angioplasty (PTCA) was performed in four of the eight pigs in the proximal left anterior descending coronary artery using standard guidewire and balloon technique with fluoroscopic guidance. Coronary artery injury was created using a standard PTCA balloon (balloon/artery ratio 1.2:1). Fluoroscopy with injection of contrast immediately after balloon deflation confirmed distal blood flow and vessel patency. After the procedure, the carotid arteriotomy was repaired with standard techniques or ligated if repair was not possible. The neck wound was closed with interrupted sutures, and the animals were returned to quarters for observation. At 28 d, the animals were killed with an intravenous commercial euthanasia solution (10 mL, Sleepaway; Fort Dodge Laboratories).

Polymer injection and specimens dehydration. After death and removal of the heart, glass cannulae were immediately tied into the coronary ostia and injected with 500 mL of heparinized saline (0.9% sodium chloride with 5,000 units of heparin) at a pressure of 70 mm Hg to clear the coronary network of blood. The anterior cardiac vein was ligated to exclude adventitial venular supply from the left anterior descending coronary arteries. A specially prepared, low-viscosity, radiopaque liquid polymer compound (MV-122; Canton Biomedical Products, Boulder, Colorado) was injected through the cannula. Polymer infusion was continued until the injected mass flowed freely from the arterial vent. The heart was then immersed in 10% neutral buffered formalin and placed in refrigeration at 4°C overnight to allow polymerization of the plastic compound. On the following day, the coronary arterial segments (~2 cm long) were removed from the heart by careful dissection and placed in a 95% alcohol solution for 48 h. At successive 24-h intervals, glycerin immersion was used, and the concentration raised from 30%, 50%, and 75% by volume. Pure glycerin was finally used to completely dehydrate the coronary segments. The specimens were then rinsed in acetone, and left in open air for 24 h. The coronary segments were embedded in wax and then in bioplastic molds for scanning and 3-D reconstruction.

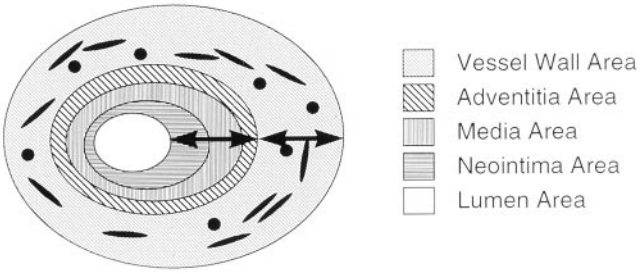

Figure 1. Schematic drawing of micro-CT reconstructed coronary artery cross-section. The vessel wall area was defined as a radius twice the distance from the arterial lumen to the outer adventitia. See text for details.

Microscopic 3-D computed tomography (CT) reconstruction. Specimens were scanned by a micro-CT system consisting of a spectroscopy x-ray tube, a fluorescent crystal plate, a microscopic objective and a charge coupled device (CCD) camera (16–18). The charge in each pixel was digitized and stored as an array in a computer as 500–1000 projections of the specimen in 360-degree rotations.

3-D images were reconstructed using a modified Feldhaup cone beam filtered back projection algorithm, and the resulting 3-D images were displayed using the Mayo Analyze software (Version 7.5; Biomedical Imaging Resource, Mayo Foundation, Rochester, Minnesota). Volume rendering provided a variety of display representations of 3-D image data sets. Volume-rendered transmission displays, maximum intensity projection and voxel gradient shading were displayed at different angles and threshold values of voxels. Average voxel size was 21–28 μm, and images of up to 800 slices were rendered for each arterial specimen (each with a matrix of 10–20-μm cubic voxels with 16 bits of gray scale).

Morphometric analysis. Seven to 10 cross-sectional images (40 normal and 32 balloon-injured cross-sections) were analyzed every 1 mm along the length of each specimen at high resolution (21-μm voxel size). A schematic diagram of this method is shown in Figure 1.

The boundary of the vessel wall was determined using a radius twice the distance from the arterial lumen to the outer

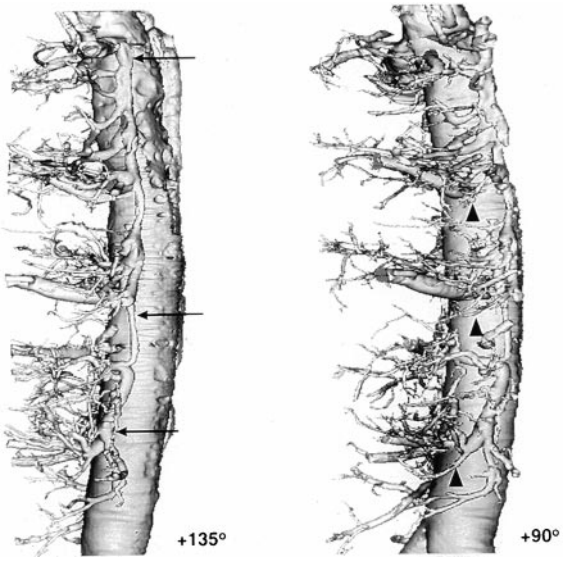

Figure 2. Voxel gradient shading of normal coronary artery shown at two different angles on the sagittal plane (voxel size, 28 μm). Two anatomically different type of vasa vasorum are visualized. First-order vasa (**arrow**) originate from the main lumen of the coronary artery (**arrow**) running longitudinally along the adventitial surface of the artery. Second-order vasa (**triangle**) originate directly from the first-order vasa, and form a plexus circumferentially around the vessel wall, as arch arterioles.

adventitia (5). The blood vessels within this boundary were defined as vasa vasorum. Blood vessels in this region were differentiated from nonvascular structures by setting voxel intensity threshold values that yielded the best discrimination as judged independently by two operators (HMK, GS). Two different measurements of vasa vasorum were computed in the analysis. First, the spatial density of vasa (vasa/mm^2) was calculated by manually counting the number of vasa and dividing by the total area of the vessel wall. Second, the total area of vessel wall occupied by blood vessels was calculated by digitally counting the number of voxels containing contrast. This area was divided by the total number of voxels within the vessel wall (summed pixel area vasa vasorum/pixel area vessel wall $\times$100).

Two anatomically different types of vasa vasorum were identified (19) (Fig. 2): first-order vasa vasorum originated from the coronary artery lumen and ran longitudinally to the coronary artery. Second-order vasa vasorum originated from first-order vasa or branches and ran circumferentially to the lumen, as arch arterioles. The number and diameter of these vessels were counted and measured separately.

After visualizing the 3-D pattern of vasa vasorum, the following morphometric variables were calculated: 1) vessel (coronary artery) wall area, 2) number and density of vasa vasorum per square millimeter of coronary artery area; 3) density ratio of first to second-order vasa vasorum; 4) percent luminal stenosis; and 5) vasa size, taken as the mean minimal diameter of first- and second-order vasa vasorum. The minimal diameter was chosen in order to avoid artifacts due to distortion of vessels not perpendicular to the imaging plane, which would be imaged as elliptical in configuration. In addition, branching points were intentionally excluded since these sites could be a source of variation in density.

After micro-CT reconstruction and analysis, the specimens were immersed for 4 h in 40°C water to gently melt the wax embedding, then removed from the plastic mold and cut every 2 mm. They were stained with hematoxylin-eosin and elastic van Gieson stain. The number of vasa in the vessel wall area was determined in histologic cross-sections for correlation with corresponding micro-CT cross-sectional images.

Statistical analysis. Data were presented as mean ± SEM, and analyzed using unpaired t tests to establish differences among groups. Correlations between the continuous variables were analyzed using a linear regression model. A value of $p < 0.05$ was considered significant in all analyses.

Results

Maximum intensity projection and voxel gradient shading images showed that in normal uninjured coronary artery, the vasa vasorum originated from branch points, connected with the main coronary artery lumen at regular intervals, and ran longitudinally along the vessel wall. These vessels were identified as first-order vasa vasorum. In both normal and injured cases, these microvessels gave rise to smaller branches running circumferentially in a plexus around the vessel wall. These latter microvasculature were defined as second-order vasa vasorum (Figs. 2 and 3).

Balloon-injured coronary arteries showed thickened vascular walls, neointimal hyperplasia at the stenotic lesion sites and substantial angiogenesis by 28 d. In particular, a dense plexus of microvessels was frequently observed in the adventitia, but did not penetrate to the media layer (Fig. 4). Such plexi were not found in normal coronary arteries. Despite significant neointimal formation 28 d after balloon injury, no neovascularization was observed in the neointima tissue itself. This was evident by the absence of neointimal vessels, and a distinctly lower x-ray density of neointimal tissue (Fig. 5).

Morphometric data for normal and injured coronary segments are summarized in Table 1. Vessel wall area was significantly smaller in normal coronary arteries compared with injured arteries (4.86 ± 0.35 mm^2 vs. 11.24 ± 0.32 mm^2, $p = 0.0001$, respectively). The density of vasa vasorum was increased in injured coronary arteries compared with normal, uninjured vessels (3.16 ± 0.17 per mm^2 vs. 1.90 ± 0.06 per mm^2, $p = 0.0001$; Fig. 6A). Additionally, there was a shift in the density ratio of first- to second-order vasa between normal (ratio 1.5) and injured coronary arteries (ratio 0.25; $p < 0.001$, respectively; Fig. 6B), suggesting that the newly formed vessels arose mainly as second-order vasa vasorum. The mean diameter of normal first-order vasa vasorum was 160.92 ± 5.10 μm and of second-order vasa, 67.99 ± 2.72 μm ($p < 0.0001$). By

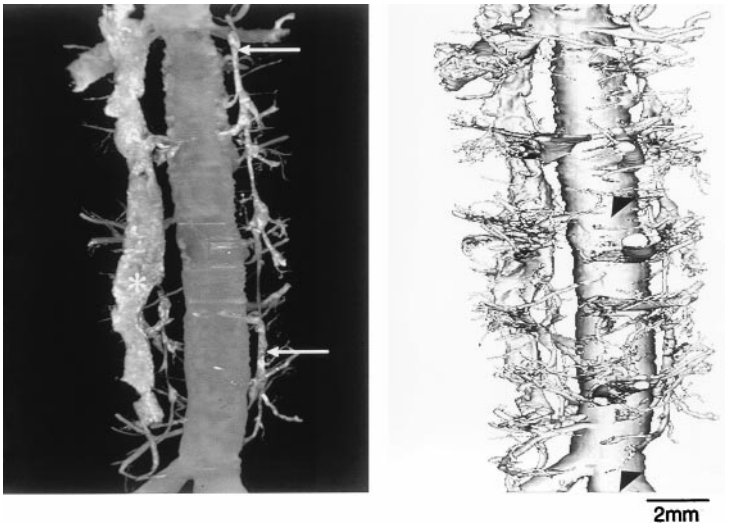

Figure 3. Maximum intensity projection and voxel gradient shading from a normal pig coronary artery demonstrated different origination and spatial distribution of vasa vasorum (voxel size, 28 μm). First-order vasa vasorum are indicated by **white arrows**. Second-order vasa vasorum are indicated by **black triangles**. A coronary vein is also visualized (**asterisk**).

comparison, the mean diameter of first-order vasa in injured coronary arteries was 141.11 ± 5.87 μm and in second order vasa 101.59 ± 1.49 μm ($p < 0.001$). These diameter differences were statistically significant between first-order and second-order vasa in normal and injured coronary arteries ($p = 0.012$, first-order; $p < 0.001$, second-order). The decrease in percent of vessel wall area comprised of vasa for balloon-injured compared with normal coronary arteries was also statistically significant (3.83 ± 0.20% vs. 5.42 ± 0.56%, $p = 0.018$).

A highly significant correlation was found between the number of vasa vasorum and percent luminal stenosis in balloon-injured coronary arteries ($r = 0.81$, $p < 0.0001$) (Fig. 7A). For example, Figure 7B shows the number of vasa vasorum and the percent stenosis along the entire length of a single balloon-injured coronary artery. As stenosis severity increased, so did the number of vasa vasorum ($r = 0.88$, $p = 0.0001$) for this vessel.

Micro-CT cross-sectional images showed good correspondence with histologic images. A significant correlation was found between the number of vessels in micro-CT cross sectional analysis and those found in histologic cross sections ($r = 0.76$, $p = 0.008$; Fig. 8).

Discussion

Several studies have examined the adventitia of coronary arteries and found fine vessel networks (1,2,14). Until now, however, no method could easily quantitate these vasa vasorum using a detailed morphological approach. The time-intensive nature and limited spatial resolution of two-dimensional histologic techniques preclude sophisticated analyses of the course of these vessels. Using the micro-CT technique, our study showed the 3-D anatomy of vasa vasorum in both normal and balloon-injured coronary arteries. Two principal conclusions may be reached from these results. First, two anatomically distinct vasa vasorum types were found in normal pig coronary arteries. First-order vasa vasorum originated from the lumen of the coronary artery and ran longitudinally along the medial-adventitial border. Second-order vasa vasorum were smaller, and arose from branches of first-order

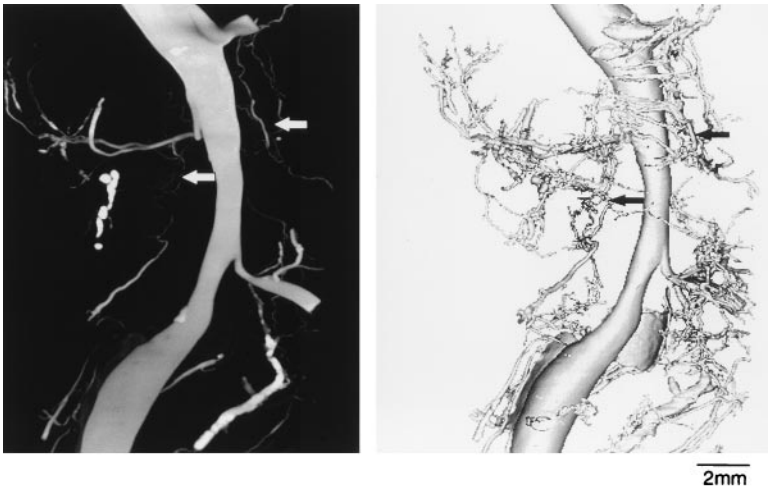

Figure 4. Maximum intensity projection and voxel gradient shading from a porcine coronary artery 28 d after balloon injury (voxel size, 28 μm). In the outer region of the vessel wall, in correspondence with the site of lumen stenosis due to neointimal hyperplasia, a dense plexus of newly formed vasa vasorum is present. First-order vasa vasorum are indicated by **white arrows**. Second-order vasa vasorum are indicated by **black triangles**.

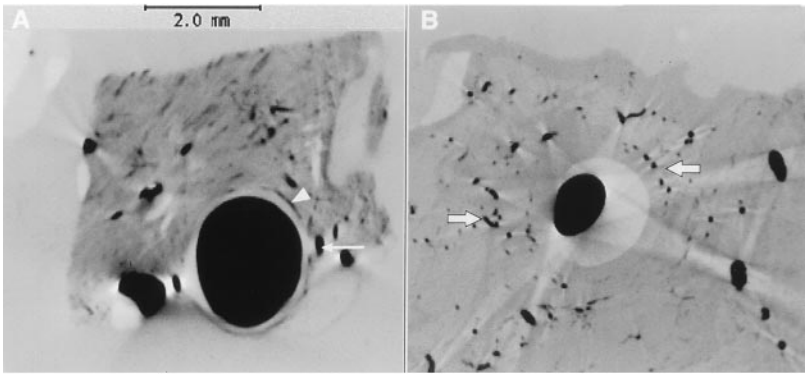

Figure 5. High-resolution micro-CT cross-sectional images from normal **(A)** and balloon-injured **(B)** porcine coronary arteries (voxel size, 21 μm). Vasa vasorum are present in the outer region of the vessel wall. Note the thickened vessel wall and significant angiogenesis 28 d after balloon injury. A distinct lower x-ray density within the main lumen indicates neointimal tissue. No neovascularization is present in the neointima itself. First-order vasa vasorum are indicated by **arrows** and second-order vasa vasorum by **triangle**.

vasa. They then separated, forming circumferential arches around the vessel wall. The second conclusion quantitates the response of vasa vasorum after balloon injury. Marked adventitial neovascularization occurred in these porcine coronary arteries by 28 d after balloon injury. These vessels were principally second-order (circumferential) vasa vasorum. While the absolute number of vasa vasorum increased, the total area of vasa was reduced in injured compared with normal coronary arteries, suggesting a decrease in vessel size that was confirmed by direct measurement. Importantly, the density of these new vasa correlated closely with stenosis severity. Furthermore, despite significant neointimal formation 28 d after balloon injury, no neovascularization was found in the neointima layer itself.

The coronary artery wall receives nutrients by outward diffusion from the lumen and inward diffusion from adventitial vasa vasorum (1,20–22). Barger et al. described vasa vasorum in human coronary arteries and found neovascularization in regions of atherosclerotic plaque (14). These authors hypothesized that human atherosclerosis might be initiated by vasa occlusion and subsequent vessel wall hypoxia acting as a stimulus for smooth muscle cell proliferation. A recent study noted a correlation between the development of new vasa and atherosclerotic disease in support of this hypothesis (23). By this hypothesis, loss of coronary artery vasa during atherosclerosis regression might account for decreased vessel wall thickness. This in turn may restore nutrient diffusion from the adventitia and coronary artery lumen (15). The role of the vasa vasorum and neovascularization might thus have fundamental, but as yet unclear roles in the pathogenesis of the arterial response to injury. While an association seems clear, a cause and effect relationship is uncertain.

Recent observations show that balloon angioplasty produces deep medial injury and adventitial stretch in both human and porcine coronary arteries (9,11,24,25). However, little is known about injury to the vasa vasorum, subsequent neovascularization and its relationship to remodeling and the growth

Table 1. Results of Quantitative Computerized Digital Analysis of Micro-CT Images by Normal and the Balloon-injured Coronary Arteries

	Normal (n = 40)	Balloon injury (n = 32)	p Value
Vessel wall area (mm^2)	4.86 ± 0.35	11.24 ± 0.32	< .001
Number density of vasa (No. vasa/mm^2)	1.90 ± 0.06	3.16 ± 0.17	< .001
Ratio of 1st/2nd-order vasa in cross-section	3:2	1:4	< .001
Mean minimal diameter of 1st-order vasa (μm)	160.92 ± 5.10	141.11 ± 5.87	0.012
Mean minimal diameter of 2nd-order vasa (μm)	67.99 ± 2.72	101.59 ± 1.49	< .001
Total area of vasa vasorum	0.21 ± 0.01	0.42 ± 0.02	< .001
Area density of vasa (%)	5.42 ± 0.56	3.83 ± 0.20	0.0185
Lumen stenosis (%)	—	43.48 ± 2.32	< .001

Figure 6. A, Vasa vasorum density between normal and balloon-injured coronary arteries. A significant increase in the density of vasa vasorum is present 28 d after balloon injury. **B,** Density ratio of first- **(open bars)** and second-order vasa vasorum **(hatched bars)** between normal and balloon-injured coronary arteries. Twenty-eight days after PTCA there was a shift in the ratio of first- to second-order vasa vasorum.

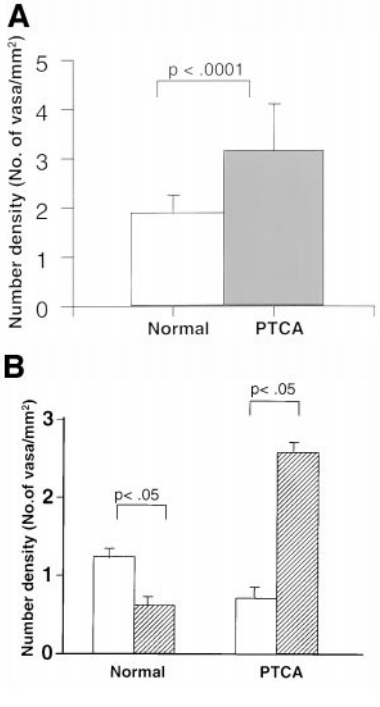

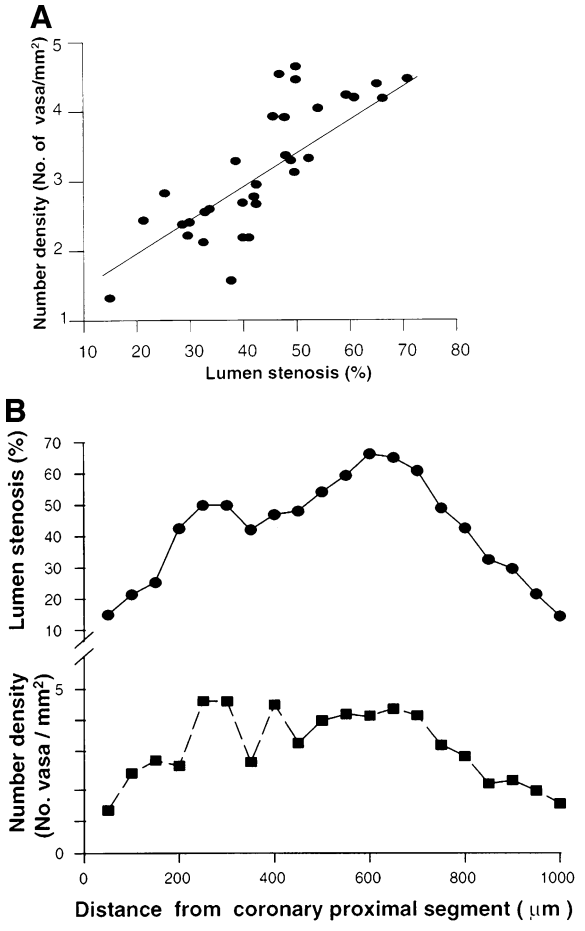

Figure 7. A, Linear regression analysis between percentage lumen stenosis and density of vasa vasorum in porcine coronary arteries after PTCA ($n = 32$, $r = 0.81$, $p < 0.0001$). **B**, Percentage lumen stenosis and the corresponding density of vasa vasorum along the entire length of a single coronary segment. In this example, as the stenosis severity increased, so did the vasa vasorum density ($r = 0.88$, $p = 0.0001$).

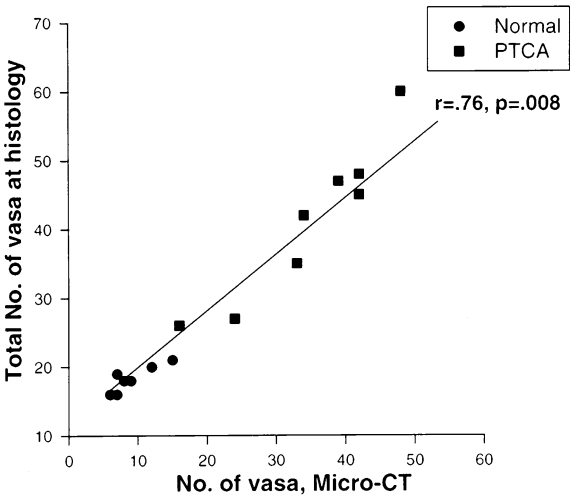

Figure 8. Linear regression analysis between cross-sectional total number vasa vasorum evaluated by micro-CT and total number vasa vasorum evaluated by histologic analysis. A significant correlation is present, indicating a good correspondence between the two techniques.

of neointimal hyperplasia. The current study shows neovascularization 28 d after balloon injury in porcine coronary arteries. Prior studies showed that neointimal thickening is proportional to the degree of injury (26). The current study extends this observation by showing that the number of vasa vasorum is directly proportional to the degree of arterial injury, determined by the thickness of neointimal hyperplasia. Whether adventitial angiogenesis is a cause or an effect of neointimal thickening, and which occurs first, are unclear but under investigation. Moreover, the implications for restenosis therapy are important. It is important to know, for example, whether angiogenesis after angioplasty could be inhibited or enhanced to achieve therapeutic effect.

Although the cause and effect question remains uncertain between neointima and angiogenesis, our results agree with prior studies where adventitial removal or serious injury caused endothelial loss and stimulated neointimal hyperplasia (27–29). In many species, as the intimal thickness exceeds the critical 0.5 mm, the layers of the vessel wall become vascularized, with a correlation between intimal hyperplasia and vasa vasorum formation (20). Therefore, it is possible that the newly formed vasa occur after the development of intimal hyperplasia. The increased number of vasa vasorum from baseline to 28 d does not seem to affect the result of angioplasty regarding neointimal hyperplasia. This 28-d time period may be insufficient to allow complete revascularization of the injured area, and a longer time period may be necessary for complete revascularization and possible regression of neointimal hyperplasia. Such a phenomenon may occur in patients, and long-term angiographic studies suggest regression of neointimal thickness over time in some cases (30,31). If the hypothesis that angiogenesis and neovascularization limits neointimal hyperplasia is correct, it may be due to reversing wall hypoxia. Alternatively, interfering with the arterial blood supply by antiangiogenic therapy immediately after injury might also induce degeneration of neointimal tissue, as suggested by regression studies of atherosclerotic plaque (15,28).

Analysis of the vessel wall and the number of vasa vasorum may explain the correlation between angiogenesis and neointimal formation. Despite increased vasa vasorum after balloon injury, the percentage of the vessel wall area covered by the newly formed vessels was reduced compared with normal coronary arteries. This finding could be due either to an increase in vessel wall area or to a decrease in size of the newly formed vasa. As outlined in the morphometric analysis, both an increase in the vessel wall area and a shift in the ratio of first- to second-order vasa in balloon-injured coronary arteries occurred.

Booth et al. developed an animal model for rapid production of focal intimal hyperplasia subsequent to perivascular manipulation by placing a polymer collar around rabbit carotid arteries (3). In rabbit carotid arteries, Barker and colleagues

(28) found that adventitial removal stimulated smooth muscle cell proliferation 7 to 14 d after injury. Regression of the intimal lesions was achieved by an artificial adventitia, using loosely placed PVC tubing, with an associated highly vascular "neoadventitia."

One possible mechanism for neovascularization after adventitial injury may be release of mitogenic substances. Shi et al demonstrated that myofibroblast migration and proliferation occurred in the adventitia after balloon injury (10). Vascular smooth muscle cell and endothelial mitogens also stimulate angiogenesis (32–36). In one study, Edelman et al. found that basic fibroblast growth factor (bFGF) increased smooth muscle cell proliferation (5). The in vivo mitogenic and angiogenic potential of bFGF was coupled to and modulated by the products of local injury. More recently, Fukuo et al. (35) demonstrated nitric oxide release from vascular smooth muscle cells induced by bFGF stimulation, with neovascularization and consequent endothelial cell proliferation.

Limitations. The principal limitation of this study stems from the sample size being small. This is a necessity given the time-intensive nature of the micro-CT scanning, reconstruction and quantitative analysis process. As more data are accumulated, continued study of the vasa vasorum will enable comparison of larger sample numbers.

Another limitation of the study related to the assumption that the polymer contrast material completely filled the microvasculature of the vessels after injection. Microscopic examination, and indeed the 3-D images, suggest that this is not a major problem since careful evaluation in both cases has not shown microvessels that were not filled with contrast. Such channels should appear empty by histopathologic examination, and as low density spaces by the micro-CT images.

A final limitation of the study relates to the use of the pig coronary artery as an animal model. These porcine coronary arteries did not have atherosclerotic plaque, and thus may not well model the human scenario of PTCA at sites with atherosclerosis. It is not possible to draw conclusions about human coronary arteries after PTCA until sufficient human lesions that underwent angioplasty become available for micro-CT examination and study.

Conclusions. Marked neovascularization by vasa vasorum occurred in porcine coronary arteries after balloon injury. The density of vasa increased proportionally to stenosis severity. This finding suggests that knowledge of the pathophysiologic significance of the adventitial vasa vasorum may determine a rational approach to limitation of neointimal formation after vessel injury. The results of this study underscore in several ways the apparent importance of the blood supply to the artery itself. Substantially more investigation is necessary to determine whether modifying growth vasa vasorum will have therapeutic effects on neointimal hyperplasia after coronary artery injury.

We thank Denise A. Reyes and Patricia E. Beighley for the expert technical assistance.

References

1. Wolinsky H, Glagov S. Nature and species differences in the medial distribution of aortic vasa vasorum in mammals. Cir Res 1967;20:409–21.
2. Barker SGE, Talbert A, Cottam S, Baskerville PA, Martin JF. Arterial intimal hyperplasia after occlusion of the adventitial vasa vasorum in the pig. Arterioscler Thromb 1993;13:70–7.
3. Booth RFG, Martin JF, Honey AC, Hassall DG, Beesley JE, Moncada S. Rapid development of atherosclerotic lesions in rabbit carotid artery induced by perivascular manipulation. Atherosclerosis 1989;76:257–68.
4. Martin JF, Booth RFG, S. M. Arterial wall hypoxia following thrombosis of the vasa vasorum is an initial lesion in atherosclerosis. Eur J Clin Invest 1991;21:355–9.
5. Edelman ER, Nugent MA, Smith LT, Karnovsky MJ. Basic fibroblast growth factor enhances the coupling of intimal hyperplasia and proliferation of the vasa vasorum in injured rat arteries. J Clin Invest 1992;89:465–73.
6. Ribeiro SMF, Schultz-Cherry S, Ullrich JE. Heparin-binding vitronectin up-regulates latent TGF-b production by bovine aortic endothelial cells. J Cell Science 1995;108:1553–61.
7. Brookes P, Clark R, Cheresh D. Requirement for vascular integrin $\alpha v\beta 3$ for angiogenesis. Science 1994;264:569–71.
8. Drake CJ, Cheresh DA, Little CD. An antagonist of integrin $\alpha v\beta 3$ prevents maturation of blood vessels during embryonic neovascularization. J Cell Science 1995;108:2655–61.
9. Shi Y, Pieniek M, O'Brien J, Mannion J, Zalewski A. Adventitial remodeling after coronary arterial injury. Circulation 1996;93:340–8.
10. Shi Y, O'Brien JE, Fard A, Mannion JD, Wang D, Zalewski A. Adventitial myofibroblasts contribute to neointimal formation in injured porcine arteries. Circulation 1996;94:1655–64.
11. Sangiorgi G, Farb A, Carter CJ, Edwards WD, Virmani R, Schwartz RS. Contribution of neointima and adventitia to the creation of final lumen area in human coronary arteries treated by balloon angioplasty. J Am Coll Cardiol 1997;29:742–2 (Abstr).
12. Heistad DD, Armstrong ML. Blood flow through vasa vasorum of coronary arteries in atherosclerotic monkeys. Arteriosclerosis 1986;6:326–31.
13. Pisco JM, Correia M, Esperanca-Pina JA, Sousa LA. Changes in the vasa vasorum following percutaneous transluminal angioplasty in a canine model of aortic stenosis. J Vasc Interv Radiol 1994;5:561–6.
14. Barger AC, Beeuwkes R, Lainey LL, Silverman KJ. Hypothesis: Vasa vasorum and neovascularization of human coronary arteries. N Engl J Med 1984;310:175–7.
15. Williams JK, Armstrong ML, Heistad DD. Vasa vasorum in atherosclerotic coronary arteries. Responses to vasoactive stimuli and regression of atherosclerosis. Circ Res 1988;62:515–23.
16. Flannery BP, Dickman HW, Roberge WG, D'Amico KL. Three-dimensional x-ray micro tomography. Science 1987;237:1439–44.
17. Avula RTV, Dunsmuir JH, Beighley PE, Thomas PJ, Faridani A, Ritman EL. A micro tomographic technique enhanced by novel image reconstruction algorithm: application to rat coronary vessels. FASEB J 1994;8:854 (Abstr).
18. Ritman EL, Dunsmuir JH, Faridani A, Finch DV, Smith KT, Thomas PJ. Local reconstruction applied to x-ray tomography. In: Chavent G, Papanicolaou G, Sack P, Symes W, eds. IMA Volumes in Mathematics and Its Applications: Inverse Problems in Wave Propagation. Vol. 90. New York: Springer-Verlag; 1997:443–52.
19. Barker SGE, Causton PA, Baskerville PA, Gent S, Martin JF. The vasa vasorum of the rabbit carotid artery. J Anatomy 1992;180:225–31.
20. Geiringer E. Intimal vascularization and atherosclerosis. J Pathol Bacteriol 1951;63:201–7.
21. Heistad DD, Marcus ML. Role of vasa vasorum in nourishment of the aorta. Blood Vessels 1979;16:225–31.
22. Werber A, Heistad DD. Diffusional support of the arteries. Am J Physiol 1985;248:H901–9.
23. Kumamoto M, Nakashima Y, Sueishi K. Intimal neovascularization in human atherosclerosis. Its origin and pathophysiological significance. Hum Pathol 1995;26:450–6.
24. Scott NA, Cipolla GD, Ross CE, et al. Identification of a potential role for the adventitia in vascular lesion formation after balloon overstretch injury of porcine coronary arteries. Circulation 1996;93:2178–87.
25. Staab ME, Srivatsa SS, Lerman A, et al. Arterial remodeling after percuta-

neous injury is highly dependent on adventitial injury histopathology. Int J Cardiol 1997;58:31–40.
26. Schwartz RS, Holmes DRJ, Topol EJ. The restenosis paradigm revisted: an alternative proposal for cellular mechanisms. J Am Coll Cardiol 1992;20: 1284–93.
27. Chignier E, Eloy R. Adventitial resection of small artery provokes endothelial loss and intimal hyperplasia. Surg Gynecol Obstet 1986;163:327–34.
28. Barker SGE, Tilling LC, Miller GC, et al. The adventitia and atherogenesis: removal initiates intimal proliferation in the rabbit which regresses on generation of "neoadventitia". Atherosclerosis 1994;105:131–44.
29. Wilcox JN, Scott NA. Potential role of the adventitia in arteritis and atherosclerosis. Intern J Cardiol 1996;54(Suppl):21–35.
30. Hermiller JB, Fry ET, Peters JF, et al. Late coronary artery stenosis regression within the Gianturco-Roubin intracoronary stent. Am J Cardiol 1996;77:247–51.
31. Mehta VY, Jorgensen MB, Raizner AE, Wolde-Tsadik G, Mahrer PR, Mansukhani P. Spontaneous regression of restenosis: an angiographic study. J Am Coll Cardiol 1995;26:696–702.
32. Cuevas P, Gonzallez AM, Carceller F, Baird A. Vascular response to basic fibroblast growth factor when infused onto the normal adventitia or into the injured media of the rat carotid artery. Circ Res 1991;69:360–9.
33. Gonzalez AM, Buscaglia M, Ong M, Baird A. Immunologicalization of basic FGF in the 18 day rat fetus: association with the basement membrane of various tissues. J Cell Biol 1990;110:347–58.
34. Folkman J, Klagsbrun M, Sasse J, Wadzinski MG, Ingber D, Vlodavsky I. A heparin-binding angiogenic protein-basic fibroblast growth factor-is stored within basement membrane. Am J Pathol 1988;130:393–400.
35. Fukuo K, Inoue T, Morimoto S, Nakahashi T, Yasuda O, Kitano S, Sasada R, Ogihara T. Nitric oxide mediates cytotoxicity and basic fibroblast growth factor release in cultured vascular smooth muscle cells: a possible mechanism of neovascularization in atherosclerotic plaques. J Clin Invest 1995;95: 669–76.
36. Bar Shavit R, Benezra M, Eldor A, Hy-Am E, Fenton JW, Wildner JD, Vlodavsky I. Thrombin immobilized to extracellular matrix is a potent mitogen for vascular smooth muscle cells: non-enzymatic mode of action. Cell Regul 1990;1:453–63.